LETTERS
PUBLISHED ONLINE: 20 JANUARY 2013 | DOI: 10.1038/NMAT3543
nature materials

# Adapting granular materials through artificial evolution

Marc Z. Miskin* and Heinrich M. Jaeger

**Over 200 years after Coulomb's studies[1], a general connection between the mechanical response of a granular material and the constituents' shape remains unknown[2–10]. The key difficulty in articulating this relationship is that shape is an inexhaustible parameter, making its systematic exploration infeasible. Here we show that the role of particle shape can, however, be explored efficiently when granular design is viewed in the context of artificial evolution[11]. By introducing a mutable representation for particle shapes, we demonstrate with computer simulation how shapes can be evolved. As proof of principle, we predicted motifs that link shape to packing stiffness, discovered a particle that produces aggregates that stiffen—rather than weaken—under compression, and verified the results using three-dimensional printing. More generally, our approach facilitates the exploration of the role of arbitrary particle geometry in jammed systems, and invites the discovery and design of granular matter with optimized properties.**

As particle shape determines both the packing arrangement[6,7,12–14] and the network of contact interactions in a granular material[4,5,9,10], selecting a particular particle shape can select a particular mechanical response. As a concrete example, compare the compressive stress–strain response for particles consisting of one, two and three equal-size rigidly bonded spheres (Fig. 1). In each case, the particles were randomly packed into a cylindrical enclosure and confined by equal pressure from all axes (Fig. 1a). This materials test, known as triaxial compression, is widely used for granular materials and standard in soil mechanics[15].

The 2-sphere particles provide both a stiffer and significantly stronger packing than the single spheres, although the stress–strain curves otherwise seem similar (Fig. 1b). Some of this improvement is caused by the neck at the point where two spheres are joined, enabling some interlocking[8,16]. However, by going to 3-sphere particles it becomes clear that the situation is more complex. For these particles, shape can be characterized by a single parameter, the opening angle at the central sphere, $\theta$. Figure 1c shows simulation results for the average elastic modulus $E$ as a function of $\theta$. Although the overall trend—that is compact particle shapes give rise to stiffer packings than extended rod-like shapes—is intuitive, it is remarkable that even modest changes in the opening angle produce significant changes in $E$. The resulting rugged landscape, full of local extrema, illustrates that, beyond corrugation originating from necks, a key role is played by the overall particle geometry. These numerical findings are confirmed by experiments on packings of three-dimensional (3D)-printed copies of the granular molecules (Fig. 1b,c), confined and compressed under conditions similar to those of the simulations (see Methods and Supplementary Methods).

The intricate relationship between the geometry of individual particles and the properties of the aggregate emerging already for very simple shapes gives a hint of both the possibilities and the complexities. The latter are compounded by the fact that further factors play a strong role. In particular, initial conditions such as packing density and loading history, as well as boundary conditions such as the confining pressure, are relevant[17]. For example, the elastic moduli of random sphere packings scale with the average number of sphere–sphere contacts, which, for frictionless elastic particles, is set by the confining pressure[9,10]. Yet this does not have to be the case for particles that can entangle and form strong packings even without external confinement[18].

Moreover, varying these parameters can alter the locations or even presence of extrema. For example, if the friction coefficient is lowered from a physical value to zero, the extrema in the three-sphere stiffness landscape fade into noise (Supplementary Fig. S1). Accordingly, boundary conditions, material parameters, and particle geometry must all be considered together to compute a physical response.

As a consequence, at present there are no general rules to predict the behaviour of a packing as particle shape is modified. Simulations can start to address this issue, but in trying to explore—and exploit—the role of particle shape, the problem faced is the overwhelming size of the search space. The key task, therefore, is to find a way to parse the vast space of possible shapes efficiently, taking account of both the desired goal and the given boundary conditions. In this Letter we introduce a new approach that achieves this.

We make headway by rephrasing the above task: select from the infinite number of potential configurations those shapes which are appropriately adapted to generate a particular behaviour, using only the capacity to check the quality of designs. Written this way, the process seems similar to biological natural selection. In fact, efficient solutions to search-and-optimization tasks of this kind often come from the field of evolutionary computing[11,19]. Here, the key concept is that starting with an initial population of objects, the best performance by a member of the population can be iteratively improved by selecting the fittest objects, mutating them to create offspring, and using the offspring to produce a subsequent generation.

Evolutionary computing has been applied successfully to a wide range of engineering problems[11,20] and is emerging as a tool for scientific discovery, for example, for crystal structure prediction[21]; however, so far it has not been used for the optimization of granular materials. Presumably this is owing to the absence of a particle-shape representation that is both unrestrictive and amenable to mutation. To solve this, we developed a shape representation that we call a blueprint. In the same way as a picture is represented by pixels, we represent an arbitrary shape as a volume composed of

James Franck Institute and Department of Physics, The University of Chicago, Chicago, Illinois 60637, USA. *e-mail: mmiskin@uchicago.edu.

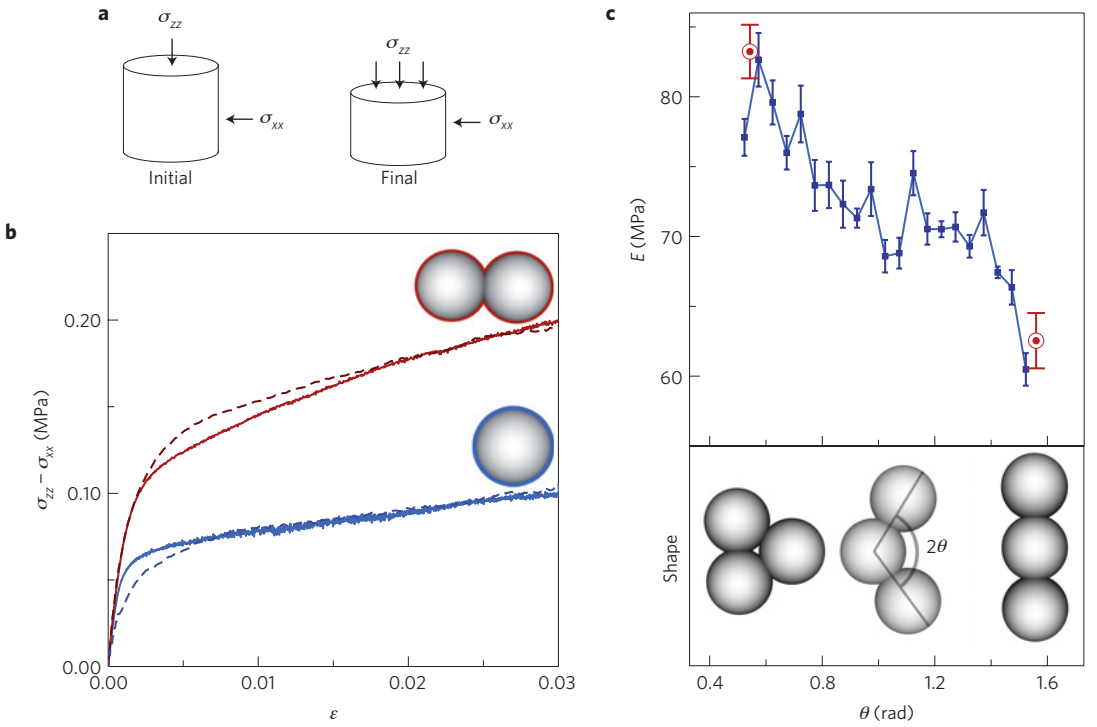


**Figure 1 | The impact of particle shape on mechanical response. a**, Sketch of a triaxial test procedure. A cylindrical volume of granular material is prepared by confining it with pressures $\sigma_{xx} = \sigma_{yy} = \sigma_{zz}$. This defines the initial condition of strain $\varepsilon = 0$. The material is then compressed along the vertical, $z$ direction. **b**, Changing the particles from single spheres to dimers consisting of two rigidly connected spheres increases the stiffness and failure stress of the material significantly both in experiment (3D-printed particles, solid curves) and in simulations (dashed curves). **c**, The rugged, nonlinear relationship between shape and stiffness for particles made from three adjoined spheres. For such trimers the full range of shapes can be parameterized by the opening angle $\theta$, as indicated. The two red data points correspond to the shapes shown below on the left and right; their abscissas were identified as extrema by our algorithm, and the ordinate values were determined experimentally. Error bars correspond to the standard deviation from 10 (4) trials for the simulations (experiments).

smaller building blocks. Abstractly, we define a blueprint as a list of bearings written in sequential order specifying where to place each building block as the compound object is being constructed. For this list of directions to define a single object, we add the rule that each new part is always added along its bearing at the furthest distance that leaves it still connected to the structure built during the previous steps.

To demonstrate the principle, in the following we use equal-size spheres as the building blocks, bonding them together to form rigid compound particles that we term granular molecules. This use of glued, slightly overlapping spheres extends earlier work that represented non-spherical particles in simulations of granular friction[16,22]. It has the computational advantage that contacts among neighbouring molecules in the packing involve only a single type of sphere–sphere interaction[22,23].

A proof by deconstruction shows that blueprint rules are general enough to approximate any object from a basic set of building blocks and that there exists a path of mutations which will morph one object into another (see Supplementary Discussion). We can use each blueprint as a genotypic expression for shape, and evolve populations by mutating the bearing angles. Each genotype can then be mapped uniquely to a particular phenotype for testing, as illustrated by Fig. 2. Importantly, this approach also minimizes the dimensionality required by the parameter space: because each block is constrained to remain connected to the built object, only two variables rather than three spatial coordinates are needed to uniquely specify its location.

In benchmark tests, we found this shape representation highly efficacious. For instance, using standard evolutionary algorithms[19] we were able to evolve initial, random sphere configurations into rings, rods, deltahedra, or cubes in typically no more than a few hundred generations (see Supplementary Discussion). It should be noted that our approach is general enough to be easily extended to different building block types. For instance, using cubes might prove useful in stochastic assembly[24]. Alternatively, keeping spheres as the building blocks, the lines adjoining overlapping

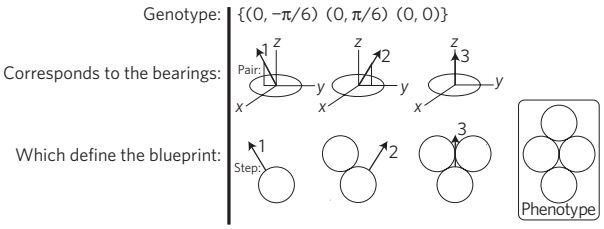


**Figure 2 | Representing particle shapes with blueprints.** To construct a single shape from a genotype of angle pairs ($n = 4$ particle represented by three angle pairs in the example shown here), the angles are first mapped to bearings in spherical coordinates. A first sphere is then placed. This sphere will act as the origin and all bearing vectors will be drawn out originating from the centre of this sphere. The remaining spheres are placed iteratively as follows. For each bearing, a ray is drawn that emanates from the centre of the origin sphere and is parallel to the bearing. If a sphere is then slid through its centre along this ray from infinitely far away towards the origin, then, the location it first comes in contact with the built structure defines the furthest distance along the bearing that still leaves it connected to the previously built shape. By taking each bearing in sequence, and placing a sphere at these distances, a phenotype shape can be constructed and used in simulations.

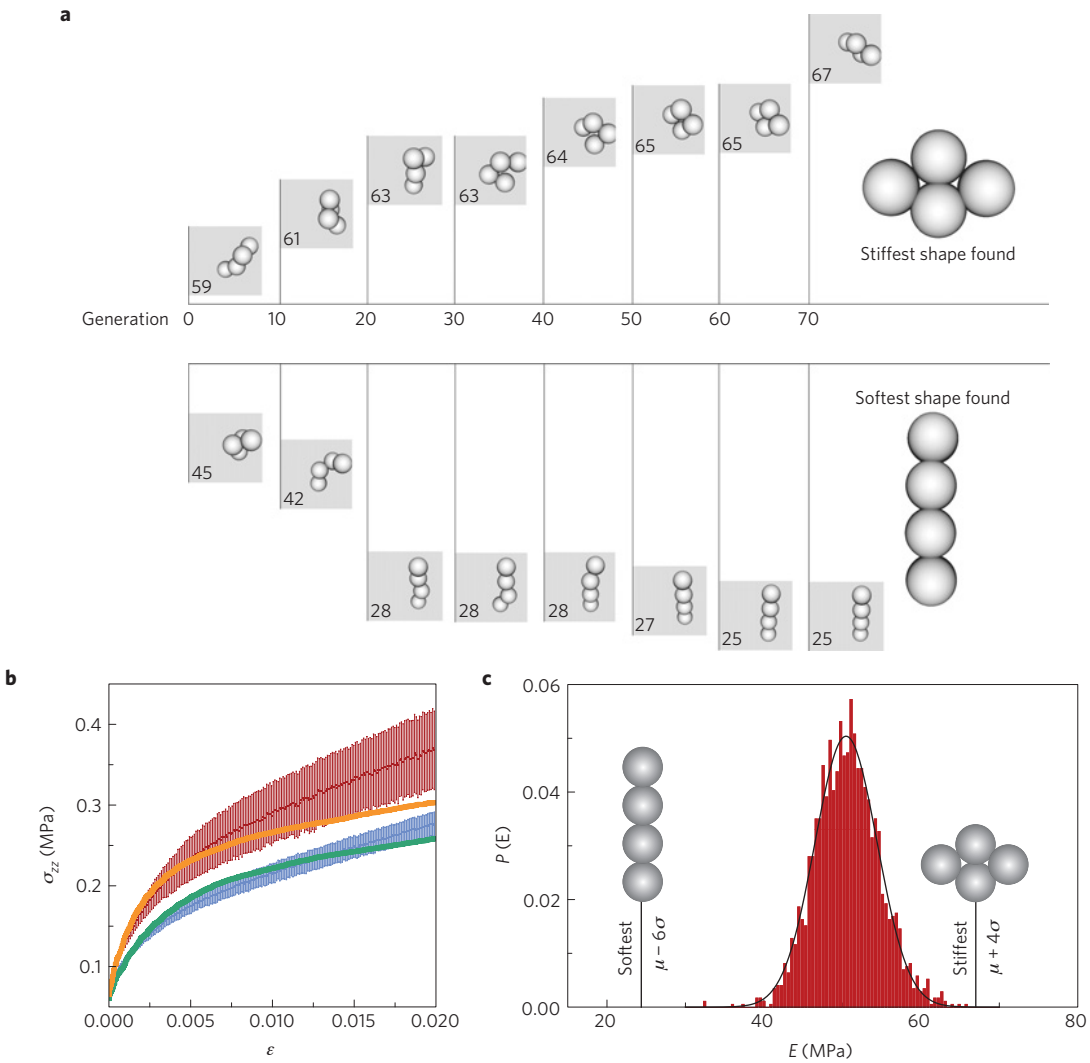


**Figure 3 | Evolving particle shapes to obtain the stiffest and softest packings.** Shown are examples using particles built from $n = 4$ spheres. Starting with a random shape, the evolution process is iterated over ~70 generations, converging to optimized shapes. **a**, Snapshots of those parent shapes that produce, in the generations indicated, the packings with the largest (smallest) elastic modulus. The vertical position of the images is scaled to the value of $E$, which is also indicated in the lower left corner of each grey box. **b**, Comparison between packings of 3D-printed particles and predicted stress–strain curves shows excellent agreement in the low-strain regime where the elastic modulus was optimized. At larger strains the data for the stiffest (orange) and softest (green) shapes start to deviate from the experimental results (red and blue, respectively; error bars correspond to the standard deviation from four independent experiments). **c**, Histogram of elastic moduli obtained with random blueprints. The line is a fit to a Gaussian with mean 50 MPa and standard deviation 4 MPa. Comparison with the shapes found in **a** demonstrates the efficiency of the evolutionary approach over random search: to discover the stiffest and softest shapes would take roughly 15,000 and 500,000,000 guesses, respectively, rather than the ~600 actually used.

spheres could be used to define beams and the same blueprint could be mapped to truss structures. Spherical building blocks can also be used directly for energy or moment optimization of colloidal particle configurations[25,26]. In fact, optimization results for the densest packings of $n$ particle clusters[27] are included in the Supplementary Discussion.

Applying this evolutionary approach to jammed particle packings, we initially consider two related goals: to find the particle shapes that produce packings with the stiffest response or the softest response to compressive loading. That is, shapes which produce packings with the largest (smallest) elastic modulus near zero strain. For granular molecules consisting of three spheres, the search converged on the configurations producing the extrema in $E$ found earlier by varying $\theta$ directly (Fig. 1c), in excellent agreement also with the experimental data (shown in red). For 4-sphere molecules, Fig. 3a shows the history of the parent shapes leading to the convergent results for each goal.

After our algorithm converged on the optimized $n = 4$ shapes, we again used 3D printing to construct physical packings and verified the results with triaxial tests. In Fig. 3b we plot the resulting stress–strain curves. The general agreement of the simulations with the experiments asserts that rejected shapes were, indeed, suboptimal. Further, the significant differences between the shapes producing the stiffest and softest responses suggest that the evolutionary algorithm makes full use of the available configuration space. Figure 3c emphasizes this point with a histogram of simulated elastic moduli for $n = 4$ genotypes using random blueprints. The stiffest and softest moduli are found at 4 and 6 standard deviations from the mean, respectively, demonstrating that the evolutionary approach to granular design is both accurate and efficient.

To strengthen this claim, we also printed and tested one suboptimal shape for $n = 4$. Specifically, we printed the last shape discovered by the algorithm before the rapid approach to straight

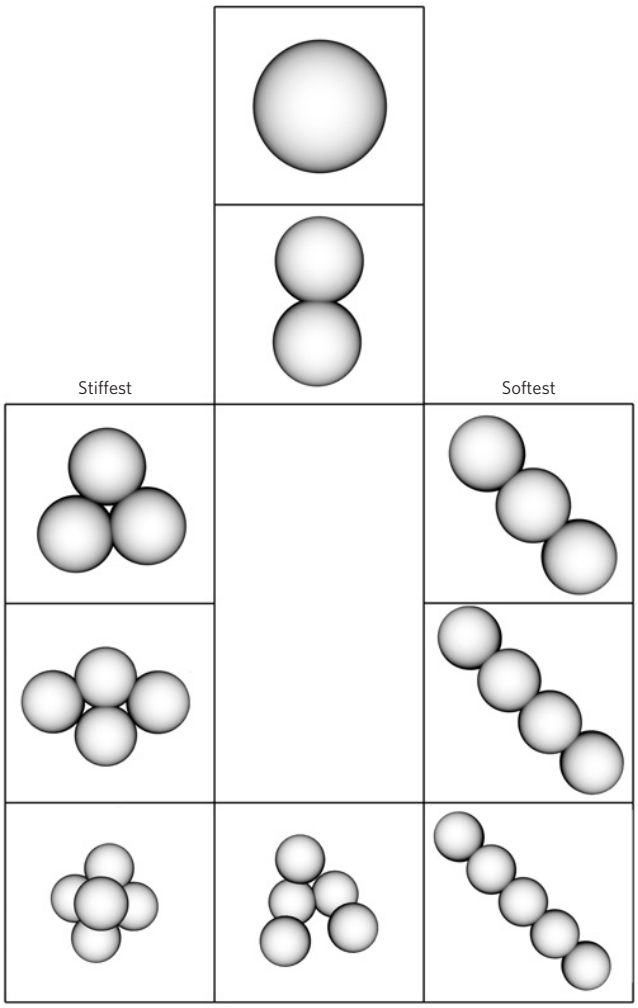


**Figure 4 | Stiffest and softest particle shapes built from spheres up to $n = 5$.** Two clear motifs emerge. First, the softest shapes discovered are always rods. Second, the stiffest $n$-shape can be constructed by taking the most compact $(n+1)$-shape and removing a single sphere. Note that the stiffest shape for $n = 4$, obtained from the $n = 5$ triangular bipyramid, is not as planar as it appears in the top view shown, but slightly bent and 'boat-shaped'. In the centre we also include our $n = 5$ strain-stiffening particle; note the asymmetry in its sphere arrangement.

shapes at 20 generations (Fig. 3b). Whereas the stiffest shape had a modulus of 67 MPa and the softest a modulus of 25 MPa, this shape was predicted by simulation to have a modulus of 46 MPa. The experimental packings were measured to have a modulus of $47 \pm 1$ MPa, in excellent agreement. The resulting stress–strain curves are included as Supplementary Fig. S6.

Repeating the optimization process to uncover the stiffest and softest shapes up to $n = 5$ causes clear motifs underpinning the optimized designs to emerge (Fig. 4). Over this range in $n$, the softest shapes discovered are always linear molecules. By contrast, the stiffest shapes are highly compact. Specifically, we find that the $n$ stiffest shape can be constructed by taking the most compact $n + 1$ shape—that is, the shape whose configuration of $n + 1$ spheres minimizes the sum of their distances to the centre of mass—and removing a sphere (see Supplementary Information). For example, the most compact shape for $n = 5$ is the triangular bipyramid[27]. Removing one sphere produces the slightly bent, approximately rhombic shape, discovered independently as the $n = 4$ stiffest shape (see Supplementary Fig. S2). Presumably, as $n$ becomes very large, the potential to evolve larger scale geometric structures will marginalize the significance of removing one sphere, and this trend is likely to break down. However, within the scope of this study, this motif is surprisingly persistent. We believe that the lucidity of these motifs makes them useful for applications and provides a first step towards the rational selection of granular shapes.

We emphasize that particle shapes producing the stiffest load response are not necessarily the ones that pack most densely. Granular materials resist stress because particles are impeded from sliding past one another, and thus the nature of the local contacts matters as well. The socket-like hole produced by removing one sphere from the most compact $(n + 1)$-shape seems to provide a local packing environment where two contacting $n$-shapes can share a sphere and lock together. For relative movement, the lock must first be undone. Linear granular molecules, on the other hand, can only form weaker connections, and contacts between overlapping rods are more susceptible to torque.

The link between contact locking and stress response invites more exotic design goals. For example, in packings near the jamming point, prior work has shown that the potential mobility of a given contact can depend strongly on the geometry of the particle[28]. Now, suppose a material was initially in a state characterized by weak particle contacts, but as these contacts were broken, new contacts formed that were stronger. Such material would stiffen the further it was compressed, in contrast to the strain softening common for granular materials (Figs 1b and 3b; note that in triaxial tests the lateral confinement is not via a hard, immobile wall, but via a surface held at constant pressure). We used our algorithm to search for appropriate shapes; that is, shapes producing the largest second derivative of stress with respect to strain. The evolutionary strategy in this case led to the discovery of a unique, asymmetric particle that, with just five constituent spheres, produces a concave-upward dependence for $\sigma(\varepsilon)$ (Fig. 5a). This strain-stiffening behaviour differs qualitatively from the stress–strain relationship found in ordinary granular materials under the same confinement conditions.

Strain-stiffening was recently found also in packings of granular polymers (linear chains of flexibly linked beads) if the polymers were long enough[18]. However, the wishbone-like granular molecule in Fig. 5a is not only rigid but also smaller—that is, consists of fewer spheres—than granular polymers that strain stiffen. This relatively small molecule achieves remarkable self-confinement under load: it can sustain stress levels ten times larger than the confining pressure (Fig. 5b). We also note that these packings exhibit a low modulus, yet do not fail up to 10% strain—an order of magnitude larger than simple spheres under the same conditions.

Despite its simplicity, the evolutionary strategy for finding particle shapes introduced here provides considerable flexibility and control. When $\sigma(\varepsilon)$ is expanded as a Taylor series in strain, our results demonstrate that shape, for given boundary conditions, can tune both the first-order (Fig. 3) and second-order (Fig. 5) terms. Beyond evolving shape with respect to only certain features of $\sigma(\varepsilon)$, such as $E$, a straightforward extension could find the best match to a full stress–strain curve. Although we focused on the stress response, optimizing with respect to geometrical properties such as a packing's porosity is of course also possible. Future work could allow the evolution process more freedom, by treating the number of building blocks or their size as directly mutable parameters, or by co-evolving within the same packing environment particle shapes that emphasize particular behaviours, such as those in Fig. 4.

We believe that this approach can be adapted to optimize the properties of any material composed of identical objects left to self-assemble. As discussed so far, only steric interactions between athermal granular molecules were considered, but it would be straightforward to use simulations that include attractive

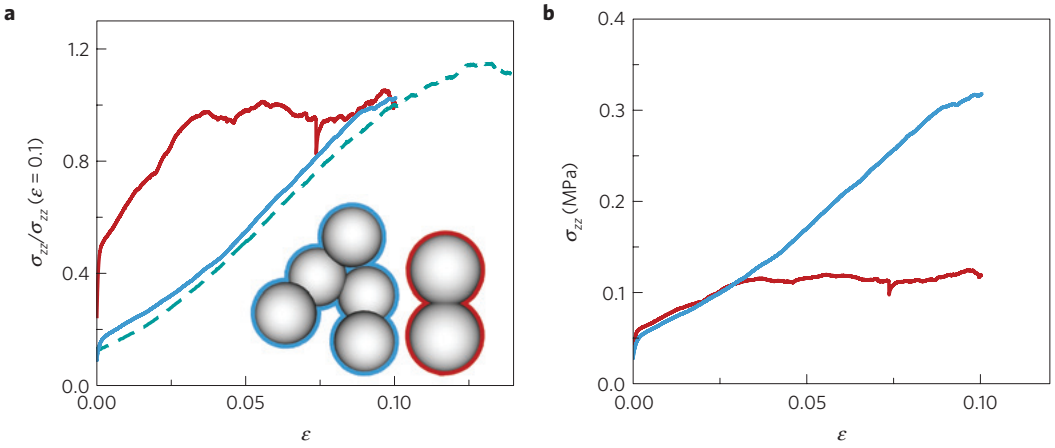


**Figure 5 | Strain stiffening. a**, Stress–strain curves for a $n = 5$ particle shape designed to strain-stiffen (simulation: green-dashed; experiment: blue-solid). The confining pressure $\sigma_{xx} = \sigma_{yy}$ for these experiments had to be reduced to 35 kPa to prevent damage to the wishbone-shaped, 3D-printed particles. Therefore, we normalized the stress axis to compare simulations (calibrated for $\sigma_{xx} = 85$ kPa) to experiments. Note the presence of a new inflection point, which leads to positive curvature, in contrast to what occurs for all other shapes that strain-soften, exemplified here by experimental data on dimer particles under 35 kPa confinement (red). **b**, Packings formed by the strain-stiffening shape are strong as well as tough. As the non-normalized data show, the failure stress is roughly a factor of three larger than for dimers under the same conditions, and it exceeds the confining pressure by an order of magnitude. This contrasts with packs of individual spheres, where the failure stress is comparable in magnitude to the confining pressure (Fig. 1b). At the same time, the strain-stiffening packings withstand much larger strains before failing (~10% compared with no more than a few per cent for packings of dimers and even less for single spheres (Fig. 1b)). These results demonstrate that our approach can control not just first-order, but also second-order stress–strain effects.

interactions and/or kinetic energy. For example, extra magnetic or electrostatic interactions could be explored by incorporating site-specific 'functional groups' into the molecules. As our evolution method is essentially a black box, any type of simulation that can take shapes modelled by bonded spheres as an input can be used as an engine for optimization. Within this framework, the limits to granular-materials design are then simply the limits to computation.

## Methods

We used an evolutionary algorithm based on the covariance matrix adaptation evolution strategy (CMA-ES; ref. 19). At each stage in the evolution, a generation of roughly ten particle shapes was tested in molecular dynamics simulations of ~2,000 particles under triaxial compression to ~4% strain. All MD simulations were performed using Itasca PFC3d software. The simulations used a normal-force linear contact model and the Cundall–Strack friction model. The simulation parameters were chosen in SI units to match experimentally measured values as closely as possible: the normal spring constant compressive modulus was set to 70 MPa, the normal-to-shear stiffness ratio was set to 5 and the friction coefficient was 0.25. The full details of the contact interaction laws can be found in prior work[29]. After our algorithm converged, >2,000 copies of the best shape discovered over the evolution process were printed in ultraviolet-cured plastic using an Objet 3D printer (resolution <40 μm). The diameter of the spheres making up individual particles ranged from 3 to 5 mm because they were scaled in both the simulations and printing process to keep the total volume of a particle independent of the number of spheres. The printed shapes were then loaded into a cylindrical latex sleeve (130 mm tall, 50 mm in diameter and 0.6 mm thick), confined by 85 kPa (unless noted otherwise) and compressed by an Instron materials tester at a rate of 10 mm $min^{-1}$. The error in our measurements was dominated by statistical variation inherent to random materials, and error bars were constructed by ensemble averaging the stress for a given strain over four individually loaded trials. The testing procedure, simulation calibration, and algorithm performance are detailed in the Supplementary Information.

Received 2 July 2012; accepted 10 December 2012; published online 20 January 2013

## References

1. Coulomb, C. *Mémoirs de Mathématique et de Physique* 343–384 (L'Imprimerie Royale, 1773).
2. Jaeger, H. M., Nagel, S. R. & Behringer, R. P. Granular solids, liquids, and gases. *Rev. Mod. Phys.* **68,** 1259–1273 (1996).
3. Duran, J. *Sands, Powders, and Grains: An Introduction to the Physics of Granular Materials* (Springer, 1999).
4. Pena, A. A., Garcia-Rojo, R. & Herrmann, H. J. Influence of particle shape on sheared dense granular media. *Granu. Matter* **9,** 279–291 (2007).
5. Zuriguel, I. & Mullin, T. The role of particle shape on the stress distribution in a sandpile. *Proc. R. Soc. Lond. A* **464,** 99–116 (2008).
6. Haji-Akbari, A. *et al.* Disordered, quasicrystalline and crystalline phases of densely packed tetrahedra. *Nature* **462,** 773–777 (2009).
7. Torquato, S. & Jiao, Y. Dense packings of the Platonic and Archimedean solids. *Nature* **460,** 876–879 (2009).
8. Schreck, C. F., Xu, N. & O'Hern, C. S. A comparison of jamming behavior in systems composed of dimer- and ellipse-shaped particles. *Soft Matter* **6,** 2960–2969 (2010).
9. Liu, A. J. & Nagel, S. R. The jamming transition and the marginally jammed solid. *Annu. Rev. Condens. Matter Phys.* **1,** 347–369 (2010).
10. Van Hecke, M. Jamming of soft particles: Geometry, mechanics, scaling and isostaticity. *J. Phys. Condens. Matter* **22,** 033101 (2010).
11. Eiben, A. E. & Smith, J. E. *Introduction to Evolutionary Computing* (Springer, 2003).
12. Zou, L. N., Cheng, X., Rivers, M. L., Jaeger, H. M. & Nagel, S. R. The packing of granular polymer chains. *Science* **326,** 408–410 (2009).
13. Baker, J. & Kudrolli, A. Maximum and minimum stable random packings of Platonic solids. *Phys. Rev. E* **82,** 061304 (2010).
14. Jaoshvili, A., Esakia, A., Porrati, M. & Chaikin, P. M. Experiments on the random packing of tetrahedral dice. *Phys. Rev. Lett.* **104,** 185501 (2010).
15. Wood, D. M. *Soil Behavior and Critical State Soil Mechanics* (Cambridge Univ. Press, 1990).
16. Galindo-Torres, S. A., Alonso-Marroquin, F., Wang, Y. C., Pedroso, D. & Munoz Castano, J. D. Molecular dynamics simulation of complex particles in three dimensions and the study of friction due to nonconvexity. *Phys. Rev. E* **79,** 060301 (2009).
17. Majmudar, T. S. & Behringer, R. P. Contact force measurements and stress-induced anisotropy in granular materials. *Nature* **435,** 1079–1082 (2005).
18. Brown, E., Nasto, A., Athanassiadis, A. G. & Jaeger, H. M. Strain-stiffening in random packings of entangled granular chains. *Phys. Rev. Lett.* **108,** 108302 (2012).
19. Hansen, N., Muller, S. D. & Koumoutsakos, P. Reducing the time complexity of the derandomized evolution strategy with covariance matrix adaptation (CMA-ES). *Evol. Comput.* **11,** 1–18 (2003).
20. Lipson, H. & Pollack, J. B. Automatic design and manufacture of robotic lifeforms. *Nature* **406,** 974–978 (2000).
21. Oganov, A. R., Lyakhov, A. O. & Valle, M. How evolutionary crystal structure prediction works—and why. *Accounts Chem. Res.* **44,** 227–237 (2011).
22. Pöschel, T. & Schwager, T. *Computational Granular Dynamics: Models and Algorithms* (Springer, 2005).

23. Kodam, M., Bharadwaj, R., Curtis, J., Hancock, B. & Wassgren, C. Force model considerations for glued-sphere discrete element method simulations. *Chem. Eng. Sci.* **64,** 3466–3475 (2009).
24. Tolley, M. T. & Lipson, H. On-line assembly planning for stochastically reconfigurable systems. *Int. J. Robot. Res.* **30,** 1566–1584 (2011).
25. Arkus, N., Manoharan, V. N. & Brenner, M. P. Minimal energy clusters of hard spheres with short range attractions. *Phys. Rev. Lett.* **103,** 118303 (2009).
26. Hoy, R. S., Harwayne-Gidansky, J. & O'Hern, C. S. Structure of finite sphere packings via exact enumeration: Implications for colloidal crystal nucleation. *Phys. Rev. E* **85,** 051403 (2012).
27. Sloane, N. J. A., Hardin, R. H., Duff, T. D. S. & Conway, J. H. Minimal-energy clusters of hard-spheres. *Discrete Comput. Geom.* **14,** 237–259 (1995).
28. Papanikolaou, S., O'Hern, C. S. & Shattuck, M. D. Isostaticity at frictional jamming. Preprint at http://arxiv.org/abs/1207.6010 (2012).
29. Potyondy, D. O. & Cundall, P. A. A bonded-particle model for rock. *Int. J. Rock Mech. Mining Sci.* **41,** 1329–1364 (2004).

## Acknowledgements

We thank E. Brown, J. Ellowitz, S. Nagel, S. Waitukaitis and T. Witten for insightful discussions, and A. Athanassiadis and M. Collins for help with the 3D-printed particles. We would like to acknowledge and thank the Itasca Education Partnership (Itasca Consulting Group) for the contribution of software and technical support. This work was supported by the NSF through its MRSEC program (DMR-0820054) and by the US Army Research Office through grant W911NF-12-1-0182.

## Author contributions

M.Z.M. and H.M.J. conceived the study and wrote the paper. M.Z.M. created the particle-shape representation, performed the simulations and experiments and analysed the data.

## Additional information

Supplementary information is available in the online version of the paper. Reprints and permissions information is available online at www.nature.com/reprints. Correspondence and requests for materials should be addressed to M.Z.M.

## Competing financial interests

The authors declare no competing financial interests.